Loading as a design parameter for genetic circuits*

Nithin Senthur Kumar[1] and Domitilla Del Vecchio[1]

Abstract— **A significant problem when building complex biomolecular circuits is due to context-dependence: the dynamics of a system are altered upon changes to its context, potentially degrading the system's performance. Here, we study retroactivity, a specific type of context-dependence, by analyzing the effects of loads on a transcription factor applied by the transcription factor target sites. In particular, we study this loading effect on the model of an activator-repressor oscillator, an important motif in synthetic biology. Our analysis indicates that strong activation and weak repression are key for a stable limit cycle. Repression can be effectively weakened by adding load to the repressor, while activation can be effectively weakened by adding load to the activator. Therefore, loading the repressor can be employed as a design parameter to establish a stable limit cycle. In contrast, loading the activator is deleterious to the clock.**

I. INTRODUCTION

Modularity is the property that allows components to be designed independently such that their input/output behavior remains unchanged upon interconnection with other modules. Modularity is, however, not universal and the dynamics of engineering systems typically change when loaded. Recently, it has been experimentally shown that biomolecular systems, such as genetic circuits, experience these loading effects [1]-[2], also called retroactivity [3]. Several types of simple biomolecular circuits and motifs, such as the toggle switch [4]-[6], gene oscillators [7]-[9], and logic gates [10]-[11] have been modularly designed and experimentally validated, and a major challenge in synthetic biology is to combine these modules to construct complex circuits [12] for applications including biofuel technology [13], biosensors [14], and various medical technologies [15]-[16].

To address the deleterious effects of retroactivity that cause modularity to fail, insulation devices have been designed to be placed between upstream and downstream systems to act as a buffer. Such devices include using high gain negative feedback [3], [17] and time scale separation [2], [18]. However, retroactivity can be viewed as an additional design parameter and in fact, all natural systems have some form of load. Signal transduction networks often regulate many downstream gene targets and in gene transcription networks, transcription factors often have many DNA sites to which they bind. Many of these sites do not even have regulatory functionalities [19], and therefore it is plausible that they are being used to tune the level and temporal dynamics of transcription factors [1].

*This work was supported by NIH P50 GM098792

[1]Nithin Senthur Kumar and Domitilla Del Vecchio are with the Department of Mechanical Engineering, MIT, 77 Massachusetts Avenue, Cambridge MA. nskumar@mit.edu, ddv@mit.edu

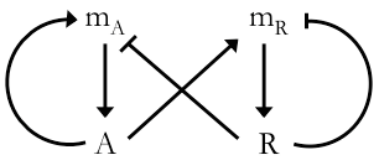

Fig. 1. Diagram of a synthetic gene oscillator with A and R representing the activator and repressor protein, respectively. A activates (arrow) m_A and m_R. R represses (bar arrow) m_R and m_A.

Recent theoretical work has considered the effect of loading on synthetic biological circuits and networks. It has been theoretically shown that loading a genetic clock through the use of additional DNA promoter binding sites can switch it on or off and also enable frequency tuning [19]. Retroactivity has been shown to affect the relative stability of toggle switches, enabling the engineering of biased switches [20]. The loading effects due to intramodular and intermodular connections leading to internal, scaling, and mixing retroactivity are studied in [21]. In this paper, we consider the activator-repressor clock built in [9]. In particular, we identify parametric conditions for the existence of a stable limit cycle and analyze the effect of load on the clock's dynamics with regard to activating and quenching oscillations using standard tools from dynamical systems theory.

This paper is organized as follows. In Section II, we derive a deterministic ODE model of the activator-repressor clock from biochemical reactions. In Section III, we consider a reduced system model and provide conditions for the existence of a stable limit cycle. In Sections IV and V, the effect of load to the activation and repression branches on the dynamics of the oscillator, respectively is studied.

II. MODEL

A representation of the core network of the genetic oscillator described in [9] is given in Fig. 1. The mRNA of the activator protein (A) and repressor protein (R) are denoted by m_A and m_R, respectively. Protein A positively regulates its own production by activating itself through the production of m_A and the production of R by activating m_R. Conversely, R negatively regulates its own production by repressing itself through the repression of m_R and the production of A by repressing m_A.

A deterministic ODE model can be derived from considering the biochemical reactions of activation, repression, multimerization, transcription, and translation of a generic protein (P) which, due to the symmetry of the model (both proteins are activated by A and repressed by R) can be used

to describe the evolution of the concentration of both A and R. These reactions are given by:

$$\mathrm{A} + \mathrm{A} + ... + \mathrm{A} \underset{\beta_{\mathrm{A}'}}{\overset{\beta_{\mathrm{A}}}{\rightleftharpoons}} \mathrm{A}_n, \tag{1}$$

$$\mathrm{R} + \mathrm{R} + ... + \mathrm{R} \underset{\beta_{\mathrm{R}'}}{\overset{\beta_{\mathrm{R}}}{\rightleftharpoons}} \mathrm{R}_m, \tag{2}$$

$$\mathrm{R}_m + \mathrm{DNA^P} \underset{\mathrm{d}^*}{\overset{\mathrm{a}^*}{\rightleftharpoons}} \mathrm{R}_m : \mathrm{DNA^P}, \tag{3}$$

$$\mathrm{A}_n + \mathrm{DNA^P} \underset{\mathrm{d}'}{\overset{\mathrm{a}'}{\rightleftharpoons}} \mathrm{A}_n : \mathrm{DNA^P}, \tag{4}$$

$$\mathrm{A}_n : \mathrm{DNA^P} \xrightarrow{\alpha_1} \mathrm{m_P} + \mathrm{A}_m : \mathrm{DNA^P}, \tag{5}$$

$$\mathrm{DNA^P} \xrightarrow{\alpha_2} \mathrm{m_P} + \mathrm{DNA^P}, \tag{6}$$

$$\mathrm{m_P} \xrightarrow{\kappa} \mathrm{m_P} + \mathrm{P}, \tag{7}$$

$$\mathrm{m_P} \xrightarrow{\delta} \emptyset, \tag{8}$$

$$\mathrm{P} \xrightarrow{\gamma} \emptyset. \tag{9}$$

Let A and R multimerize with cooperativity n and m, with forward rates of β_A, β_R and reverse rates of β'_A, β'_R, respectively, leading to reactions (1)-(2). Since activation and repression are assumed to take place at the transcriptional level, the complex formed by the reversible reaction (with forward rate a^* and reverse rate d^*) between $\mathrm{R_m}$ and DNA promoter ($\mathrm{DNA^P}$), denoted $\mathrm{R_m}$:$\mathrm{DNA^P}$, does not contribute to transcription and effectively sequesters free $\mathrm{DNA^P}$, as given in (3). Conversely, $\mathrm{A_n}$:$\mathrm{DNA^P}$ is the complex formed by the reversible reaction (with forward rate a' and reverse rate d') between $\mathrm{A_n}$ and $\mathrm{DNA^P}$, as shown in (4). This complex undergoes translation at rate α_1 to produce an mRNA molecule, leading to (5). The model also assumes that some transcription can occur without A bound to $\mathrm{DNA^P}$ (i.e., transcriptional leakiness), described by (6). Translation occurs at a rate κ, given in (7), and mRNA and protein decay at a rate δ and γ, respectively, given in (8)-(9). The ODE model for the mRNA and protein dynamics is given by:

$$\begin{aligned} \dot{m}_P &= \alpha_1[A_n : DNA^P] + \alpha_2[DNA^P] - \delta m_P, \\ \dot{P} &= \kappa m_P - \gamma P. \end{aligned} \tag{10}$$

Assuming the total concentration of DNA is constant, the following conservation law holds:

$$DNA_{tot} = DNA^P + [R_m : DNA^P] + [A_n : DNA^P].$$

Assuming complex formation occurs significantly faster than mRNA and protein dynamics [22], setting their respective rate equations at quasi-steady state (i.e., $\dot{A}_n, \dot{R}_m$, $[\mathrm{A_n} : \mathrm{DNA^P}], [\mathrm{R_m} : \mathrm{DNA^P}] = 0$) and solving for [$\mathrm{A_n}$:$\mathrm{DNA^P}$] and [$\mathrm{DNA^P}$] in terms of A, R yields:

$$[\mathrm{A}_n : \mathrm{DNA^P}] = \frac{\frac{a'\beta_A}{d'\beta_{A'}} DNA_{tot} A^n}{1 + \frac{a'\beta_A}{d'\beta_{A'}} A^n + \frac{a^*\beta_R}{d^*\beta_{R'}} R^m}, \tag{11}$$

$$[\mathrm{DNA^P}] = \frac{DNA_{tot}}{1 + \frac{a'\beta_A}{d'\beta_{A'}} A^n + \frac{a^*\beta_R}{d^*\beta_{R'}} R^m}. \tag{12}$$

Equation (10) represents the dynamics of a general mRNA and protein system with transcriptional activation and repression by A and R, respectively. Substituting (11)-(12) in (10) and then using the subscripts "R" or "A" to denote parameters corresponding to R or A production and decay, respectively yields the final model equations:

$$\begin{aligned} \dot{m}_A &= \frac{\alpha(A/k_A)^n + \alpha_0}{1 + (A/k_A)^n + (R/k_R)^m} - \delta_A m_A, \\ \dot{m}_R &= \frac{\alpha(A/k_A)^n + \alpha_0}{1 + (A/k_A)^n + (R/k_R)^m} - \delta_R m_R, \\ \dot{A} &= \kappa_A m_A - \gamma_A A, \\ \dot{R} &= \kappa_R m_R - \gamma_R R. \end{aligned} \tag{13}$$

The parameter $\alpha = \alpha_1 DNA_{tot}$ is a measure of the maximum transcriptional activation by $\mathrm{A_n}$:$\mathrm{DNA^P}$ to mRNA and $\alpha_0 = \alpha_2 DNA_{tot}$ represents transcriptional leakiness (or basal transcriptional expression) of mRNA. Since the promoters controlling the expression of A and R are the same, given the symmetry of the system, we can assume that α and α_0 are equal for both the $\mathrm{m_A}$ and $\mathrm{m_R}$ dynamics. The contribution of basal transcription to the production of mRNA is assumed to be small in magnitude compared to that of the promoter (i.e., $\frac{\alpha_0}{\alpha} << 1$). The parameters $k_A = (\frac{d'\beta_{A'}}{a'\beta_A})^{\frac{1}{n}}$ and $k_R = (\frac{d^*\beta_{R'}}{a^*\beta_R})^{\frac{1}{m}}$ indicate the relative affinity for complex formation. The protein translation and decay rate are given by κ and γ, respectively and the mRNA decay rate is denoted by δ.

III. Two-state approximation

Due to the time scale separation between transcription of DNA to mRNA and translation, the original four-state system (13) can be reduced to a two-state system by considering m_A and m_R at their quasi-steady state [23]:

$$m_A = \frac{1}{\delta_A} \frac{\alpha(A/k_A)^n + \alpha_0}{1 + (A/k_A)^n + (R/k_R)^m}, \tag{14}$$

$$m_R = \frac{1}{\delta_R} \frac{\alpha(A/k_A)^n + \alpha_0}{1 + (A/k_A)^n + (R/k_R)^m}. \tag{15}$$

Substituting (14)-(15) in the $\dot{A}, \dot{R}$ equations of (13) yields the two-state approximation:

$$\dot{A} = \frac{\kappa_A}{\delta_A} \frac{\alpha(A/k_A)^n + \alpha_0}{1 + (A/k_A)^n + (R/k_R)^m} - \gamma_A A = f(A, R), \tag{16}$$

$$\dot{R} = \frac{\kappa_R}{\delta_R} \frac{\alpha(A/k_A)^n + \alpha_0}{1 + (A/k_A)^n + (R/k_R)^m} - \gamma_R R = g(A, R). \tag{17}$$

To determine sufficient conditions for oscillatory behavior, the Poincaré-Bendixson theorem [24] is used to infer the existence of a stable limit cycle. This requires (i) the existence of a unique equilibrium point and (ii) that this equilibrium point is unstable and not a saddle.

Since the system is two-dimensional, analyzing the expression for the nullclines provides a convenient way of determining conditions for a unique equilibrium point. The nullclines are defined by setting $\dot{A} = 0$ and $\dot{R} = 0$ and are

given by:

$$R = k_R\left[\frac{\kappa_A}{\delta_A\gamma_A A}\left[\alpha\Big(\frac{A}{k_A}\Big)^n + \alpha_0\right] - \left(1 + \Big(\frac{A}{k_A}\Big)^n\right)\right]^{\frac{1}{m}}, \tag{18}$$

$$A = k_A\left[\frac{-\kappa_R\alpha_0 + \gamma_R\delta_R R(1 + (\frac{R}{k_R})^m)}{\kappa_R\alpha - \gamma_R\delta_R R}\right]^{\frac{1}{n}}. \tag{19}$$

Claim: If α_0 is sufficiently large, system (16)-(17) has a unique equilibrium point.

Proof: Solving for $\frac{\alpha(A/k_A)^n+\alpha_0}{1+(A/k_A)^n+(R/k_R)^m}$ in (16)-(17) and equating the resulting expressions yields:

$$\frac{\kappa_A}{\delta_A\gamma_A A} = \frac{\kappa_R}{\delta_R\gamma_R R}. \tag{20}$$

This results in the equilibrium point lying on the line defined by:

$$A = cR, \qquad c = \frac{\kappa_A\delta_R\gamma_R}{\kappa_R\delta_A\gamma_A}. \tag{21}$$

Substituting (21) in (19) yields:

$$P(R) = (\frac{k_A^n\gamma_R\delta_R}{k_R^m})R^{m+1} + (\gamma_R\delta_R c^n)R^{n+1} - (\kappa_R\alpha c^n)R^n + (k_A^n\gamma_R\delta_R)R - k_A^n\kappa_R\alpha_0 = 0. \tag{22}$$

For $n, m > 1$, the coefficients of $P(R)$ change signs three times when arranged in descending powers of R (regardless of the value of n or m). By Descartes' rule of signs, $P(R) = 0$ has either one or three positive root(s). Since the coefficient of the terms with the largest exponent (either $m+1$ or $n+1$) are always positive, as $R \to \infty$, $P(R) \to \infty$. To ensure a single positive root, it is enough to translate $P(R)$ sufficiently vertically downwards.

To this end, let R_M be any value of R sufficiently large such that there are no more inflection points for $P(R > R_M)$ and let $M = \sup_{R\in[0,R_M]} P(R)$. By the Extreme Value Theorem, M must be finite since $P(R)$ is a continuous function of R.

The parameter, α_0, which corresponds to the basal expression rate of mRNA does not appear in any of the coefficients of $P(R)$ except for the constant term. Therefore, increasing α_0 translates $P(R)$ downwards and so for any M, $P(0)$ can be set sufficiently negative so that $P(R)$ only crosses the R-axis once. This crossing corresponds to the terms with exponents of $n+1$ or $m+1$ dominating the value of $P(R)$, resulting in a unique equilibrium point. ■

Fig. 2 plots the nullclines for a small and large value of α_0, leading to a change in number of equilibrium points from 3 to 1, respectively. In the sequel, a sufficiently large α_0 was used to ensure a unique equilibrium point.

By the Poincaré-Bendixson theorem, if the equilibrium point is unstable and not a saddle point, there exists a limit cycle. Since this system approximation is two dimensional, the eigenvalues of the Jacobian matrix and the condition for the existence of a limit cycle is given as (where J is the

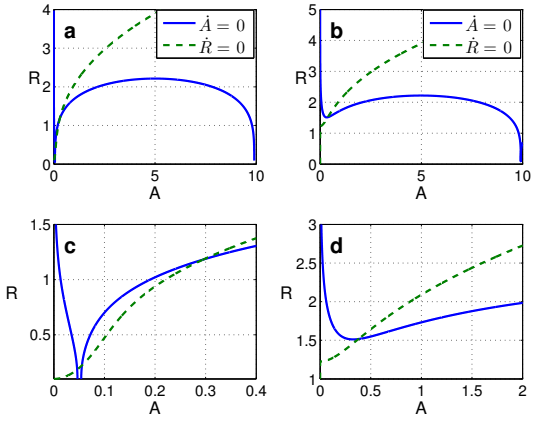

Fig. 2. System nullclines for (16)-(17) demonstrating the change in number of equilibria from 3 (**a** with closeup **c**) to 1 (**b** with closeup **d**) as $P(0)$ is made more negative (i.e., for sufficiently large α_0, the system has 1 equilibrium point). System parameter values include: $\alpha = 20\text{hr}^{-1}$, $k_A = k_R = 1\text{nM}$, $\alpha_0 = 0.05$(**ac**), 2(**bd**) nMhr^{-1}, $\delta_A = \delta_R = 1\text{hr}^{-1}$, $\kappa_A = 2\text{hr}^{-1}$, $\kappa_R = 1\text{hr}^{-1}$, $\gamma_A = 4\text{hr}^{-1}$, $\gamma_R = 0.5\text{hr}^{-1}$, $n = 2$, $m = 4$.

Jacobian matrix, Tr is trace, and det is determinant):

$$\lambda_{1,2} = \frac{Tr(J) \pm \sqrt{Tr(J)^2 - 4det(J)}}{2}, \tag{23}$$

$$Re[\lambda_{1,2}] > 0 \iff Tr(J) > 0, det(J) > 0. \tag{24}$$

The Jacobian J is given by:

$$J = \begin{bmatrix} \frac{\partial f}{\partial A} & \frac{\partial f}{\partial R} \\ \frac{\partial g}{\partial A} & \frac{\partial g}{\partial R} \end{bmatrix}\Bigg|_{(A_e,R_e)}.$$

The determinant of J is given by (evaluated at the equilibrium point):

$$det(J) = \frac{\partial f}{\partial A}\frac{\partial g}{\partial R} - \frac{\partial f}{\partial R}\frac{\partial g}{\partial A}.$$

Since $\frac{\partial f}{\partial A}, \frac{\partial g}{\partial A} > 0$ and $\frac{\partial g}{\partial R}, \frac{\partial f}{\partial R} < 0$, we have that $\frac{\partial f}{\partial A}\frac{\partial g}{\partial R}$ is always negative and $-\frac{\partial f}{\partial R}\frac{\partial g}{\partial A}$ is always positive. To see how $det(J) > 0$ can be graphically verified, we consider how these conditions translate in terms of the nullcline slopes at the equilibrium point. From (16)-(17), the nullclines satisfy:

$$f(A, R) = 0,$$
$$g(A, R) = 0.$$

Let $X_A(A), X_R(A)$ be the locally unique solution to $f(A, R) = 0$ and $g(A, R) = 0$ about the equilibrium point:

$$R = X_A(A) \implies f(A, X_A(A)) = 0,$$
$$R = X_R(A) \implies g(A, X_R(A)) = 0.$$

The nullclines are therefore defined by $R = X_A(A)$ and $R = X_R(A)$. By the Implicit Function Theorem:

$$\frac{dX_A}{dA}\bigg|_{(A_e,R_e)} = -\frac{(\partial f/\partial A)\big|_{(A_e,R_e)}}{(\partial f/\partial R)\big|_{(A_e,R_e)}},$$

$$\frac{dX_R}{dA}\bigg|_{(A_e,R_e)} = -\frac{(\partial g/\partial A)\big|_{(A_e,R_e)}}{(\partial g/\partial R)\big|_{(A_e,R_e)}}.$$

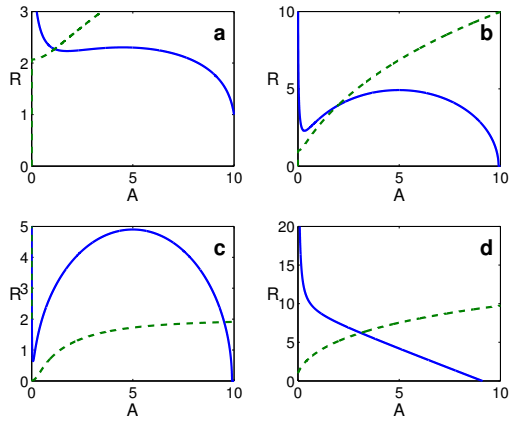

Fig. 3. Four possible nullcline intersection regions of (16) and (17) given by blue solid ($f = 0$) and green dotted lines ($g = 0$), respectively. System parameters include α = 20nMhr^{-1}, $k_A = k_R$ = 1nM, α_0 =40(**a**), 2(**b**), 0.1(**c**), 2(**d**) nMhr^{-1}, $\delta_A = \delta_R$ = 1hr^{-1}, $\kappa_A = \kappa_R$ = 1hr^{-1}, γ_A = 2hr^{-1}, γ_R =1(**abd**), 10(**c**) hr^{-1}, n =2(**abc**) 1(**d**), m =2(**abc**) 1(**d**).

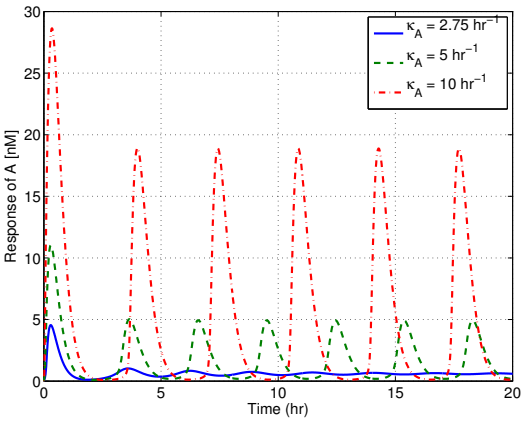

Fig. 4. Change in response of A from decaying to stable oscillations as κ_A increases for system given by (16)-(17). System parameters include α = 20nMhr^{-1}, $k_A = k_R$ = 1nM, α_0 = 2nMhr^{-1}, $\delta_A = \delta_R$ = 1hr^{-1}, κ_R = 1hr^{-1}, γ_A = 4hr^{-1}, γ_R = 0.5hr^{-1}, $n = 2$, $m = 4$.

Since $\frac{\partial f}{\partial R} < 0$ and $\frac{\partial g}{\partial R} < 0$:

$$\left.\frac{dX_A}{dA}\right|_{(A_e,R_e)} = \frac{(\partial f/\partial A)\big|_{(A_e,R_e)}}{\left|(\partial f/\partial R)\big|_{(A_e,R_e)}\right|}, \tag{25}$$

$$\left.\frac{dX_R}{dA}\right|_{(A_e,R_e)} = \frac{(\partial g/\partial A)\big|_{(A_e,R_e)}}{\left|(\partial g/\partial R)\big|_{(A_e,R_e)}\right|}. \tag{26}$$

$det(J) > 0$ requires (at the equilibrium point):

$$\frac{\partial g}{\partial A}\left|\frac{\partial f}{\partial R}\right| > \frac{\partial f}{\partial A}\left|\frac{\partial g}{\partial R}\right|,$$

that is:

$$\frac{\frac{\partial g}{\partial A}}{\left|\frac{\partial g}{\partial R}\right|} > \frac{\frac{\partial f}{\partial A}}{\left|\frac{\partial f}{\partial R}\right|},$$

which, from (25)-(26), is equivalent to:

$$\frac{dX_R}{dA} > \frac{dX_A}{dA}.$$

Therefore, the condition $det(J) > 0$ is guaranteed if the slope of the nullcline defined by $g = 0$ is larger than the slope of the nullcline defined by $f = 0$ at the equilibrium point. The four qualitatively different types of unique equilibrium points are given in Fig. 3. In Fig. 3a, 3c, 3d, the slope of $X_A(A)$ at the equilibrium point is negative. Given equality (25), this implies that $\frac{\partial f}{\partial A} < 0$. Since $Tr(J) = \frac{\partial f}{\partial A} + \frac{\partial g}{\partial R}$ and $\frac{\partial g}{\partial R} < 0$, it follows that in these cases, the equilibrium point is stable. An unstable equilibrium point can occur only when the nullclines intersect as in Fig. 3b. We therefore focus on this case in the sequel.

To determine which parameter values can make the trace positive, we observe its analytical expression which is given by:

$$Tr(J) = \frac{\alpha\kappa_A}{\delta_A}\left(\frac{n(A_e/k_A)^{n-1}[1 - \frac{\alpha_0}{\alpha} + (R_e/k_R)^m]}{k_A[1 + (A_e/k_A)^n + (R_e/k_R)^m]^2}\right) - \gamma_A - \frac{\alpha\kappa_R}{\delta_R}\left(\frac{m(R_e/k_R)^{m-1}((A_e/k_A)^n + \frac{\alpha_0}{\alpha})}{k_R[1 + (A_e/k_A)^n + (R_e/k_R)^m]^2}\right) - \gamma_R. \tag{27}$$

The last three terms are always negative. The expression for the trace suggests that it can be made positive by increasing $\frac{\kappa_A\alpha}{\delta_A}$. This ratio is the maximum production rate of A, which corresponds to having a fully active promoter (i.e., $A \to \infty$) leading to a steady-state m_A value of $\frac{\alpha}{\delta_A}$. Increasing $\frac{\kappa_A\alpha}{\delta_A}$, however, does not guarantee that the two-state system approximation exhibits sustained oscillations, since $\alpha, \kappa_A, \delta_A$ affect the value of the equilibrium point, making it difficult to identify their effect on the trace. Furthermore, increasing α would also increase the third term. Nevertheless, Fig. 4 demonstrates that increasing κ_A does lead to oscillations. For a stable limit cycle, α was set an order of magnitude larger than α_0 (corresponding to Fig. 3b) and κ_A was set sufficiently high to ensure a positive trace. Relatively large values of α_0 were found to make the equilibrium point stable (i.e., for $\alpha_0 \approx \alpha$ as in Fig. 3a).

To summarize our findings, the system given by (16)-(17) has a unique equilibrium point for sufficiently large α_0. The conditions for an unstable equilibrium point include (i) the nullclines need to intersect with positive slope at the equilibrium point (α_0 should not be too large), (ii) the slope of the nullcline defined by $g = 0$ should be greater than the slope of the nullcline of $f = 0$ at the equilibrium point, and (iii) sufficiently large maximum production rate of A (κ_A) compared to that of R.

IV. Downstream load to A

Consider A transcriptionally regulating downstream promoter sites represented schematically in Fig. 5.

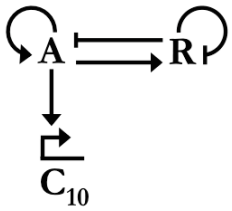

Fig. 5. Load of A by downstream promoter sites.

This transcriptional regulation occurs by A binding to the DNA promoter sites. Let the free promoter sites be denoted as C_{10} and the sites bound to A be denoted as C_{11}. Since DNA does not decay, the total concentration of promoter sites is conserved, that is $C_{10}+C_{11}=C_{t1}$, where C_{t1} represents the total concentration of the free and bound promoter sites. The complex formation reaction is given by:

$$C_{10}+A \underset{d}{\overset{a}{\rightleftarrows}} C_{11}.$$

The dynamics of A change in the new three-state system equations, which are now given by:

$$\begin{aligned}\dot{A} &= \frac{\kappa_A}{\delta_A}\frac{\alpha(A/k_A)^n+\alpha_0}{1+(A/k_A)^n+(R/k_R)^m}-\gamma_A A-\dot{C}_{11},\\ \dot{R} &= \frac{\kappa_R}{\delta_R}\frac{\alpha(A/k_A)^n+\alpha_0}{1+(A/k_A)^n+(R/k_R)^m}-\gamma_R R,\\ \dot{C}_{11} &= a(C_{t1}-C_{11})A-dC_{11}. \end{aligned} \tag{28}$$

Increased loading to A (increased C_{t1}) decreases the amplitude of oscillations to the point of quenching oscillations as shown in Fig. 6. The response of R is qualitatively similar to that of A: higher C_{t1} values cause smaller amplitude oscillations and increased frequency until the clock is quenched.

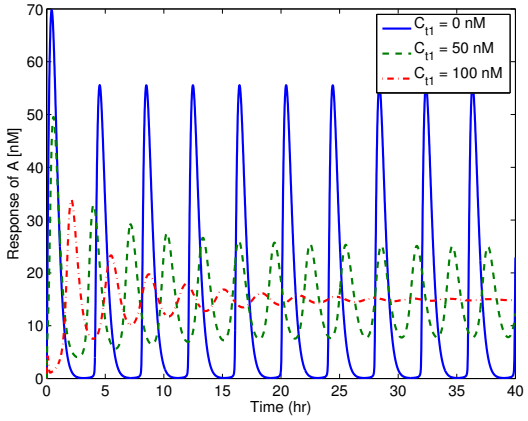

Fig. 6. Simulation of (28) with system parameters: $\alpha = 20\text{nMhr}^{-1}$, $k_A = k_R = 1\text{nM}$, $\alpha_0 = 2\text{nMhr}^{-1}$, $\delta_A = \delta_R = 1\text{hr}^{-1}$, $\kappa_A = 20\text{hr}^{-1}$, $\kappa_R = 1\text{hr}^{-1}$, $\gamma_A = 4\text{hr}^{-1}$, $\gamma_R = 0.5\text{hr}^{-1}$, $a = d = 1\text{hr}^{-1}$, $n = 2$, $m = 4$.

To understand the reason for this, we analyze how the eigenvalues of the linearized system change due to the addition of C_{t1}. To simplify the system, using the assumption that complex formation (C_{11}) occurs relatively faster than protein dynamics (A,R) [22], the three-state system can be reduced to two states. To this end, we employ singular perturbation and introduce the new (slow) variable Z, defined as $Z = A + C_{11}$. Rewrite the system by defining $\epsilon = \frac{\gamma_A}{d}$, $K_{d1} = \frac{d}{a}$, and $a = \frac{\gamma_A}{\epsilon K_{d1}}$. Substituting these expressions into (28) yields the system in standard singular perturbation form given by:

$$\begin{aligned}\dot{Z} &= \frac{\kappa_A}{\delta_A}\frac{\alpha(\frac{Z-C_{11}}{k_A})^n+\alpha_0}{1+(\frac{Z-C_{11}}{k_A})^n+(R/k_R)^m}-\gamma_A(Z-C_{11}),\\ \dot{R} &= \frac{\kappa_R}{\delta_R}\frac{\alpha(\frac{Z-C_{11}}{k_A})^n+\alpha_0}{1+(\frac{Z-C_{11}}{k_A})^n+(R/k_R)^m}-\gamma_R R,\\ \epsilon\dot{C}_{11} &= \frac{\gamma_A}{K_{d1}}(C_{t1}-C_{11})(Z-C_{11})-\gamma_A C_{11}. \end{aligned} \tag{29}$$

Setting $\epsilon = 0$ and solving for C_{11} in terms of A yields the slow manifold:

$$C_{11} = \frac{C_{t1}A/K_{d1}}{1+A/K_{d1}} = g_1(A),$$

which can be shown to be locally exponentially stable [25]. Since $Z = A + C_{11}$, we have $\dot{Z} = \dot{A} + \dot{C}_{11}$, and so:

$$\dot{Z} = \dot{A} + \frac{dg_1(A)}{dA}\dot{A}.$$

Solving for $\dot{A}$ yields:

$$\begin{aligned}\dot{A} &= \frac{\dot{Z}}{1+\frac{dg_1(A)}{dA}},\\ &= \left(\frac{\kappa_A}{\delta_A}\frac{\alpha(\frac{A}{k_A})^n+\alpha_0}{1+(\frac{A}{k_A})^n+(\frac{R}{k_R})^m}-\gamma_A A\right)\frac{(1+\frac{A}{K_{d1}})^2}{(1+\frac{A}{K_{d1}})^2+\frac{C_{t1}}{K_{d1}}}.\end{aligned}$$

The resulting reduced model of the clock with load on A is thus given by:

$$\begin{aligned}\dot{A} &= \frac{(1+\frac{A}{K_{d1}})^2}{(1+\frac{A}{K_{d1}})^2+\frac{C_{t1}}{K_{d1}}}\left(\frac{\kappa_A}{\delta_A}\frac{\alpha(\frac{A}{k_A})^n+\alpha_0}{1+(\frac{A}{k_A})^n+(\frac{R}{k_R})^m}-\gamma_A A\right),\\ \dot{R} &= \frac{\kappa_R}{\delta_R}\frac{\alpha(A/k_A)^n+\alpha_0}{1+(A/k_A)^n+(R/k_R)^m}-\gamma_R R. \end{aligned} \tag{30}$$

Note that when there is no load (i.e., $C_{t1} = 0$), we recover (16)-(17). The dynamics of R have not changed from (17). The new $\dot{A}$ equation is the product of a loading term (always positive and less than 1) and (16) and so the dynamics of A are effectively slower due to the load. The new system nullclines are identical to that of (16)-(17), since the nullcline defined by $\dot{A} = 0$ is independent of the loading term. Therefore, the equilibrium point (A_e, R_e) for the unloaded two-state system and for the loaded reduced model system is the same.

To analytically investigate what the effect of the load is on the clock's behavior, we analyze the stability of the equilibrium point for the two state system (30). Since the sign of $det(J)$ is not affected by the presence of the load, as before we can guarantee that $det(J) > 0$ by requesting that the slope of the nullcline defined by $\dot{R} = 0$ is greater than the slope of the nullcline defined by $\dot{A} = 0$ at the equilibrium point. If this is satisfied, the real part of the eigenvalues of the

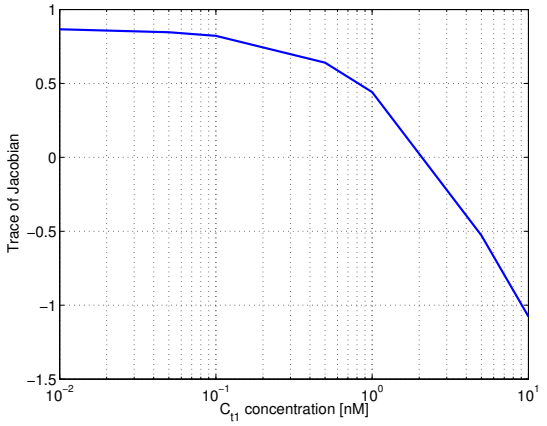

Fig. 7. Semilog plot of total promoter concentration vs trace of Jacobian for reduced system for loading to A, given by (30). System parameters include $\alpha = 20\text{nMhr}^{-1}$, $k_A = k_R = 1\text{nM}$, $\alpha_0 = 2\text{nMhr}^{-1}$, $\delta_A = \delta_R = 1\text{hr}^{-1}$, $\kappa_A = 5\text{hr}^{-1}$, $\kappa_R = 1\text{hr}^{-1}$, $\gamma_A = 4\text{hr}^{-1}$, $\gamma_R = 0.5\text{hr}^{-1}$, $n = 2$, $m = 4$.

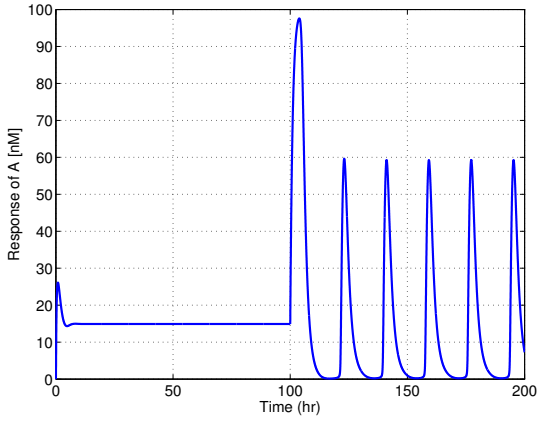

Fig. 9. Simulation of (31) demonstrating the transition from decayed response to oscillatory behavior by addition of downstream $C_{t2} = 100\text{nM}$ at $t = 100\text{hr}$. System parameters include: $\alpha = 20\text{hr}^{-1}$, $k_A = k_R = 1\text{nM}$, $\alpha_0 = 2\text{nMhr}^{-1}$, $\delta_A = \delta_R = 1\text{hr}^{-1}$, $\kappa_A = 5\text{hr}^{-1}$, $\kappa_R = 1\text{hr}^{-1}$, $\gamma_A = 1\text{hr}^{-1}$, $\gamma_R = 0.5\text{hr}^{-1}$, $a' = d' = 1\text{hr}^{-1}$, $n = 2$, $m = 4$.

reduced system can be made positive if $Tr(J) > 0$, which is given by:

$$Tr(J) = \frac{\left(\frac{\kappa_A}{\delta_A}\left(\frac{n(\frac{A_e}{k_A})^{n-1}(\alpha+\alpha(\frac{R_e}{k_R})^m-\alpha_0)}{k_A[1+(\frac{A_e}{k_A})^n+(\frac{R_e}{k_R})^m]^2}\right)-\gamma_A\right)}{1+\frac{C_{t1}/K_{d1}}{(1+A_e/K_{d1})^2}}$$
$$+\frac{\left(\frac{\kappa_A}{\delta_A}\frac{\alpha(A_e/k_A)^n+\alpha_0}{1+(\frac{A_e}{k_A})^n+(\frac{R_e}{k_R})^m}-\gamma_A A_e\right)\left(\frac{2C_{t1}}{K_{d1}^2}+\frac{2A_eC_{t1}}{K_{d1}^3}\right)}{[(1+\frac{A_e}{K_{d1}})^2+\frac{C_{t1}}{K_{d1}}]^2}$$
$$-\frac{\kappa_R}{\delta_R}\left(\frac{m(R_e/k_R)^{m-1}(\alpha(A_e/k_A)^n+\alpha_0)}{k_R[1+(\frac{A_e}{k_A})^n+(\frac{R_e}{k_R})^m]^2}\right)-\gamma_R.$$

The last line of the expression for the trace is a negative constant and independent of C_{t1}. The value of the term in the middle line is 0 since it includes the expression for $\dot{A}$ in its numerator, which is 0 when evaluated at the equilibrium point. As C_{t1} becomes larger, the magnitude of the first term decreases. Therefore, even if $Tr(J)$ is initially positive when $C_{t1} = 0$, for large enough C_{t1} the expression in the last line dominates and $Tr(J) < 0$. The change in the value of the trace as a function of C_{t1} is illustrated in Fig. 7. Therefore, for sufficiently high load to A, the system will not exhibit a limit cycle and will converge to the stable equilibrium point.

V. Downstream load to R

Now consider the case when only R has downstream load (no C_{t1}) represented schematically in Fig. 8.

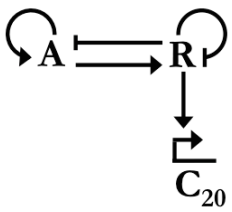

Fig. 8. Load of R by downstream promoter sites.

Let the free promoter sites be denoted as C_{20} and the sites bound to R be denoted as C_{21}. Once again, since DNA does not decay, the total concentration of the promoter sites is conserved and is given by $C_{20} + C_{21} = C_{t2}$. The complex formation reaction is given by:

$$C_{20} + R \underset{d'}{\overset{a'}{\rightleftarrows}} C_{21}.$$

The dynamics of R have changed and the three-state system equations are given by:

$$\begin{aligned}\dot{A} &= \frac{\kappa_A}{\delta_A}\frac{\alpha(A/k_A)^n+\alpha_0}{1+(A/k_A)^n+(R/k_R)^m}-\gamma_A A,\\ \dot{R} &= \frac{\kappa_R}{\delta_R}\frac{\alpha(A/k_A)^n+\alpha_0}{1+(A/k_A)^n+(R/k_R)^m}-\gamma_R R-\dot{C}_{21},\\ \dot{C}_{21} &= a'(C_{t2}-C_{21})R-d'C_{21}. \end{aligned} \quad (31)$$

We find that a quenched oscillator can be brought back to functioning by loading R with large enough promoter concentration. To demonstrate this "activation" of the gene oscillator, consider the case when the real part of the linearized system eigenvalues are negative, but close to the origin. Fig. 9 demonstrates the stable system transitioning to limit cycle behavior after $t = 100$ hr by the addition of a downstream system to R (with $C_{t2} = 100\text{nM}$). The initial two-state system, given in (16)-(17), has eigenvalues of $\lambda = -0.75 \pm 0.89j$ and the three-state system with downstream loading to R, given in (31), has eigenvalues of $\lambda = -47.31, 0.72, 23.77$.

To understand why this occurs, once again we consider how the eigenvalues of the linearized system change due to the addition of C_{t2} by assuming that complex formation (C_{21}) occurs significantly quicker than protein (A, R) dynamics for model reduction. By following a procedure similar to what was performed in Section IV, we finally reach the

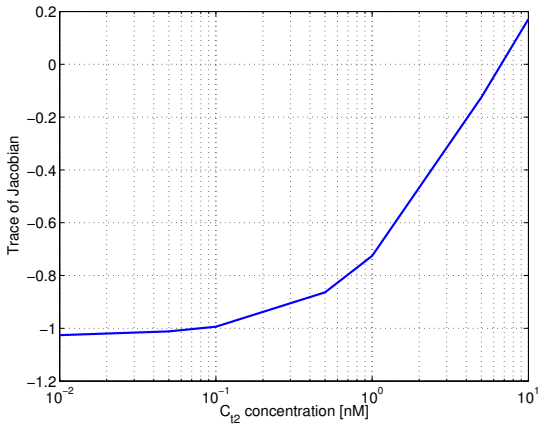

Fig. 10. Semilog plot of total promoter concentration vs trace of Jacobian for reduced system for loading to R, given by (32). System parameters include $\alpha = 20\text{nMhr}^{-1}$, $k_A = k_R = 1\text{nM}$, $\alpha_0 = 2\text{nMhr}^{-1}$, $\delta_A = \delta_R = 1\text{hr}^{-1}$, $\kappa_A = 1\text{hr}^{-1}$, $\kappa_R = 0.35\text{hr}^{-1}$, $\gamma_A = 4\text{hr}^{-1}$, $\gamma_R = 0.5\text{hr}^{-1}$, $n = 2$, $m = 4$.

following reduced two-state model:

$$\dot{A} = \frac{\kappa_A}{\delta_A}\frac{\alpha(A/k_A)^n + \alpha_0}{1 + (A/k_A)^n + (R/k_R)^m} - \gamma_A A,$$
$$\dot{R} = \frac{(1+\frac{R}{K_{d2}})^2}{(1+\frac{R}{K_{d2}})^2 + \frac{C_{t2}}{K_{d2}}}\left(\frac{\kappa_R}{\delta_R}\frac{\alpha(\frac{A}{k_A})^n + \alpha_0}{1 + (\frac{A}{k_A})^n + (\frac{R}{k_R})^m} - \gamma_R R\right). \quad (32)$$

As before, $det(J) > 0$ can be verified graphically by ensuring that the slope of the nullcline defined by $\dot{R} = 0$ is greater than that of the nullcline defined by $\dot{A} = 0$ at the equilibrium point. Furthermore, the equilibrium point remains the same since the loading term to $\dot{R}$ is always positive. The expression for the trace of the linearized system with downstream load to R is given by:

$$Tr(J) = \frac{\kappa_A\alpha}{\delta_A}\left(\frac{n(A_e/k_A)^{n-1}[1 - \frac{\alpha_0}{\alpha} + (R_e/k_R)^m]}{k_A[1 + (\frac{A_e}{k_A})^n + (\frac{R_e}{k_R})^m]^2}\right)$$
$$- \gamma_A + \frac{\left(\frac{\kappa_R}{\delta_R}\frac{\alpha(A_e/k_A)^n+\alpha_0}{1+(\frac{A_e}{k_A})^n+(\frac{R_e}{k_R})^m} - \gamma_R R_e\right)\left(\frac{2C_{t2}}{K_{d2}^2} + \frac{2R_eC_{t2}}{K_{d2}^3}\right)}{[(1+\frac{R_e}{K_{d2}})^2 + C_{t2}/K_{d2}]^2}$$
$$- \frac{\frac{\kappa_R}{\delta_R}\left(\frac{m(R_e/k_R)^{m-1}(\alpha(A_e/k_A)^n+\alpha_0)}{k_R[1+(\frac{A_e}{k_A})^n+(\frac{R_e}{k_R})^m]^2}\right) - \gamma_R}{1 + \frac{C_{t2}/K_{d2}}{(1+\frac{R_e}{K_{d2}})^2}}.$$

The first term is always positive due to the assumption that the contribution to transcription due to leakiness is significantly less than that due to A_n:DNA^P (i.e., $\frac{\alpha_0}{\alpha} << 1$). For sufficiently large $\frac{\kappa_A\alpha}{\delta_A}$, the first term is larger in magnitude than γ_A. The value of the third term is 0 since it contains the expression for $\dot{R}$, which at the equilibrium point is 0. The last term is always negative, but as C_{t2} increases, its magnitude decreases. Therefore, if the value of the trace for the two-state reduced model system with load to R is initially negative (system trajectories converge to an equilibrium point), we would expect it to become positive for sufficiently large C_{t2} as shown in Fig. 10, leading to linearized system eigenvalues with positive real part and limit cycle behavior.

VI. CONCLUSIONS

A deterministic ODE model of an activator-repressor clock was derived from biochemical reactions to determine conditions for a stable limit cycle. The effects of load on the oscillator indicate that robust, sustained oscillations are achieved when there is strong activation and comparatively weak repression. Loading provides a means to tune the relative strengths of the activation and repression branches by changing the number of downstream DNA binding sites for either the activator or repressor protein, respectively. We have shown it is possible to activate a quenched oscillator by sequestering enough repressor protein, effectively slowing repression dynamics. Similar conclusions were reached in [19], for an activator-repressor clock with no self-repression dynamics: in fact, the effect of retroactivity was found to be qualitatively similar with respect to the change in the expression of the trace of the linearized reduced model. This suggests that the qualitative behavior of genetic networks where there is interplay of positive and negative feedback may be effectively tuned by appropriately adjusting loads to the network's transcription factors.

The ability to tune the strength of the clock for stronger or weaker oscillations using additional DNA binding sites is useful in the context of synthetic circuits since it is easier to implement than changing the promoter regions or using degradation tags. Furthermore, this mechanism may already be used in natural systems: transcription factors have multiple DNA binding sites, not all of which serve regulatory functions [26]. One possible use of these binding sites could be to tune the dynamics of transcription networks.

REFERENCES

[1] S. Jayanthi, K. S. Nilgiriwala, and D. Del Vecchio, "Retroactivity controls the temporal dynamics of gene transcription," *ACS Synthetic Biology*, vol. 2, pp. 431-441, 2013.

[2] D. Mishra, P. M. Rivera, A. Lin, D. Del Vecchio, and R. Weiss, "A load driver device for engineering modularity in biological networks," *Nature Biotechnology*, vol. 32, pp. 1268-1275, 2014.

[3] D. Del Vecchio, A. J. Ninfa, and E. D. Sontag, "Modular cell biology: retroactivity and insulation," *Nature/EMBO Molecular Systems Biology*, vol. 4:161, 2008.

[4] T. S. Gardner, C. R. Cantor, and J. J. Collins, "Construction of a genetic toggle switch in Escherichia coli," *Nature*, vol. 403, pp. 339-342, 2000.

[5] D. E. Chang, S. Leung, M. R. Atkinson, A. Reifler, D. Forger, and A. J. Ninfa, "Building biological memory by linking positive feedback loops," *Proceedings of the National Academy of Sciences of the United States of America*, vol. 107, pp. 175-180, 2010.

[6] B. P. Kramer, A. U. Viretta, M. D. Baba, D. Aubel, W. Weber, and M. Fussenegger, "An engineered epigenetic transgene switch in mammalian cells," *Nature Biotechnology* vol. 22, pp. 867-870, 2004.

[7] M. B. Elowitz and S. Leibler, "A synthetic oscillatory network of transcriptional regulators," *Nature*, vol. 403, pp. 339-342, 2000.

[8] M. Tigges, T. T. Marquez-Lago, J. Stelling, and M. Fussenegger, "A tunable synthetic mammalian oscillator," *Nature*, vol. 457, pp. 309-312, 2009.

[9] J. Stricker, S. Cookson, M. R. Bennett, W. H. Mather, L. S. Tsimring, and J. Hasty, "A fast, robust and tunable synthetic gene oscillator," *Nature*, vol. 456, pp. 516-519, 2008.

[10] J. C. Anderson, C. A. Voigt, and A. P. Arkin, "Environmental signal integration by a modular AND gate," *Molecular Systems Biology*, vol. 3, pp. 133, 2007.

[11] A. Tamsir, J. J. Tabor, and C. A. Voigt, "Robust multicellular computing using genetically encoded NOR gates and chemical "wires"," *Nature*, vol. 469, pp. 212-215, 2011.

[12] D. Del Vecchio, "Modularity, context dependence, and insulation in engineered biological circuits," *Trends in Biotechnology*, 2014.

[13] H. Alper and G. Stephanopoulos, "Engineering for biofuels: exploiting innate microbial capacity or importing biosynthetic potential?," *Nature Reviews Microbiology*, vol. 7, pp. 715-723, 2009.

[14] K. J. Morey, M. S. Antunes, K. D. Albrecht, T. A. Bowen, J. F. Troupe, K. L. Havens, and J. I. Medford, "Developing a synthetic signal transduction system in plants," *Methods in Enzymology*, vol. 497, pp. 581-602, 2011.

[15] T. K. Lu and J. J. Collins, "Dispersing biofilms with engineered enzymatic bacteriophage," *Proceedings of the National Academy of Sciences*, vol. 104, pp. 11197-11202, 2007.

[16] J. C. Anderson, E. J. Clarke, A. P. Arkin, and C. A. Voigt, "Environmentally controlled invasion of cancer cells by engineered bacteria," *Journal of Molecular Biology*, vol. 355, pp. 619-627, 2006.

[17] K. Nilgiriwala, J. Jimenez, P. M. Rivera, and D. Del Vecchio, "A synthetic tunable amplifying buffer circuit in E. coli," *ACS Synthetic Biology*, vol. 4, pp. 577-584, 2015.

[18] S. Jayanthi and D. Del Vecchio, "Retroactivity attenuation in biomolecular systems based on timescale separation," *IEEE Transactions on Automatic Control*, vol. 56(4), pp. 748-761, 2011.

[19] S. Jayanthi and D. Del Vecchio, "Tuning genetic clocks employing DNA binding sites," *PLOS One*," vol. 7(7), e41019, 2012.

[20] S. M. Lyons, W. Xu, J. Medford, and A. Prasad, "Loads bias genetic and signaling switches in synthetic and natural systems," *PLoS Computational Biology*, vol. 10(3), e1003533, 2014.

[21] A. Gyorgy and D. Del Vecchio, "Modular composition of gene transcription networks," *PLoS Computational Biology*, vol. 10(3), e1003486, 2014.

[22] U. Alon, "An Introduction to Systems Biology: Design Principles of Biological Circuits," *Chapman & Hall/CRC*, 2007.

[23] BioNumbers: The database of useful biological numbers. http://bionumbers.org, 2015.

[24] I. Bendixson, "Sur les courbes définies par des équations différenetielles," *Acta Mathematica*, vol. 24(1), pp. 1-88, 1901.

[25] D. del Vecchio and R. Murray, "Biomolecular Feedback Systems," *Princeton University Press*, 2014.

[26] K. Robison, A. M. McGuire, and G. M. Church, "A comprehensive library of DNA-binding site matrices for 55 proteins applied to the complete Escherichia coli K-12 genome," *Journal of Molecular Biology*, vol. 284, pp. 241-54, 1998.